Decision Boundary Evaluation of Optimum and Suboptimum Detectors in Class-A Interference

Khodr A. Saaifan, *Student Member, IEEE,* and Werner Henkel, *Member, IEEE*

***Abstract*—The Middleton Class-A (MCA) model is one of the most accepted models for narrow-band impulsive interference superimposed to additive white Gaussian noise (AWGN). The MCA density consists of a weighted linear combination of infinite Gaussian densities, which leads to a non-tractable form of the optimum detector. To reduce the receiver complexity, one can start with a two-term approximation of the MCA model, which has only two noise states (Gaussian and impulsive state). Our objective is to introduce a simple method to estimate the noise state at the receiver and accordingly, reduce the complexity of the optimum detector. Furthermore, we show for the first time how the decision boundaries of binary signals in MCA noise should look like. In this context, we provide a new analysis of the behavior of many suboptimum detectors such as a linear detector, a locally optimum detector (LOD), and a clipping detector. Based on this analysis, we insert a new clipping threshold for the clipping detector, which significantly improves the bit-error rate performance.**

***Index Terms*—Impulse noise, non-Gaussian interference, Class-A density, decision boundaries.**

I. Introduction

IMPULSIVE interference corrupts a variety of many practical wireless systems such as radio frequency interference (RFI) in indoor and outdoor channels [1]–[3], RFI generated by computers for embedded wireless data transceivers [4], and co-channel interference in a Poisson field of interferers [5], [6]. The source of interference can be either natural or man-made such as atmospheric noise, power lines, ignition, and emissions from closely located wireless systems. Since the emissions of interfering sources and their spatial locations are randomly varying over time, the interference is well-approximated by a Gaussian distribution when the number of sources is large [7]. Otherwise, when the number of potential interfering sources is small, the interference will have a structured appearance and exhibits impulsive characteristics.

There are several distributions [3], [8]–[10] for impulse noise such as a Middleton Class-A (MCA) density, a symmetric alpha-stable (SαS) distribution, Gaussian mixture models, and a generalized Gaussian distribution. The MCA and SαS distribution are derived for Poisson distributed interferers under bounded and unbounded path-loss assumptions [3], [11], respectively. However, the unbounded path-loss assumption that is underlying the SαS distribution is not realistic [11], the MCA model appears to be more physically accurate.

Paper approved by E. Perrins, the Editor for Modulation Theory of the IEEE Communications Society. Manuscript received August 29, 2011; revised December 29, 2011 and May 24, 2012.

The authors are with the Center of Advanced Systems Engineering (CASE), Transmission System Group, Jacobs University Bremen, Bremen, 28759, Germany (e-mail: {k.saaifan, w.henkel}@jacobs-university.de).

Digital Object Identifier 10.1109/TCOMM.2012.100812.110565

Here, we restrict our attention to a classical detection problem of binary signals corrupted by MCA noise. Since the MCA model possesses an infinite number of noise states, the optimum detector has a high computational complexity. As a suboptimum solution, the linear detector, which is optimum for Gaussian noise, can be used. However, its performance degrades over a strongly impulsive channel. In [12], [13], it was shown that employing a nonlinear preprocessor improves the performance of a linear detector such as a locally optimum detector (LOD), a clipping detector, and a blanking detector. In [14]–[16], it has been shown that the MCA density can be well-approximated by two or three states of noise. Extracting the noise state at the receiver simplifies the receiver design, which motivates us to derive the decision boundaries for a two-dimensional case. Thereafter, we introduce an accurate analysis for the operations of the linear detector, the LOD [12], and the clipping detector [13]. On this basis, we propose a new clipping threshold, which minimizes the impact of the clipping nonlinearity on the correct decision regions. Compared with other adaptive clipping thresholds, we show that the proposed one has a better performance.

This paper is organized as follows. Section II briefly describes the system model, and it provides a background of the optimum and suboptimum detectors. In Section III, we introduce a simple suboptimum detector in MCA noise, which realizes the knowledge of the noise state at the receiver. Section IV presents the decision boundary analysis in the presence of MCA noise. The performance analysis of suboptimum detectors is provided in Section V. Section VI introduces and compares the proposed clipping threshold with other adaptive thresholds. Finally, simulation results and concluding remarks are presented in sections VII and VIII, respectively.

II. System Model and Background

A. System Model

We consider signal detection in the presence of impulse noise modeled by a MCA density. For simplicity, we restrict the analysis to binary phase-shift keying (PSK). However, the generalization to an arbitrary M-ary signal set is straightforward. We assume that the receiver is supplied with N replicas of the same transmitted signal, which can, e.g., be realized by transmitting the signal over different N time slots. We further assume that the transmit signal $\pm s(t)$ uses a rectangular pulse over $0 \leq t \leq T_b$. The received interference as seen by the receiver consists of additive white Gaussian noise (AWGN), $n_g(t)$, superimposed to impulse noise, $n_i(t)$, which results from the interference of various man-made or natural sources.

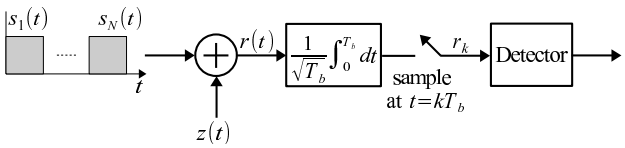

Fig. 1. System model.

Hence, the received noise is given by

$$z(t) = n_g(t) + n_i(t)\,, \tag{1}$$

where $n_g(t)$ and $n_i(t)$ are assumed to be statistically independent. At the receiver, after matched-filtering and sampling (see Fig. 1), the received signal vector $\mathbf{r} = [r_1 \cdots r_N]$ can be expressed as

$$r_k = \pm B + z_k\,, \quad k = 1, \cdots, N \tag{2}$$

where $B = \sqrt{E_s} = \sqrt{\frac{E_b}{N}}$ and z_k is the noise sample at the k^{th} sampling instant

$$z_k = \frac{1}{T_b}\int_{(k-1)T_b}^{kT_b} z(t)dt\,. \tag{3}$$

Since the impulsive characters of noise are due to the existence of interference from various sources, we make the following assumptions on the interference similar to [3]:

1) There is an infinite number of potential sources in the interference source domain.
2) The interference waveforms comprising $n_i(t)$ have the same form. However, their envelopes, duration, frequencies, and phases are randomly distributed.
3) The locations of interfering sources and their emission times are randomly distributed in space and time according to a homogeneous Poisson point process.
4) Due to the path-loss, the received power of interference is inversely proportional to $d^{2\gamma}$, where d is the distance from the source of interference to the receiver and γ is the attenuation factor.

When the mean duration of the interference waveforms T_i is comparable to the bit duration T_b, the noise samples z_k at the output of the receive filter can be modeled by an MCA density as [3]

$$p(z_k) = \sum_{m=0}^{\infty} \alpha_m g(z_k; 0, \sigma_m^2)\,, \tag{4}$$

where

$$\alpha_m = \frac{\mathrm{e}^{-A}A^m}{m!}\,, \tag{5}$$

$$g(z;\mu,\sigma_m^2) = \frac{1}{\sqrt{2\pi\sigma_m^2}}\mathrm{e}^{-\frac{(z-\mu)^2}{2\sigma_m^2}}\,, \tag{6}$$

$$\sigma_m^2 = \frac{N_0}{2}\cdot\frac{m/A+\Gamma}{1+\Gamma}\,, \tag{7}$$

and N_0 is the noise power spectral density. This model has two basic parameters A and Γ. The impulsive index, A, is defined by $A = \lambda T_i$, where λ is the rate of a homogeneous Poisson point process that governs the generation of the interfering waveforms. The impulsive index is used to measure the channel impulsiveness, e.g., at small values of A, the statistics of the output samples are characterized as a summation of a few interfering waveforms and the interference has an impulsive appearance. For a large number of interferers, i.e., $A \gg 1$, the noise statistic is almost Gaussian. The Gaussian factor Γ_k is the power ratio of a Gaussian to a non-Gaussian component of noise during the k^{th} time slot. Under a locally stationary noise assumption [3], there are no changes regarding average source numbers and emission properties during the N time slots. Therefore, the Gaussian factors are identical, i.e., $\Gamma_k = \Gamma$, $\forall k = 1, \cdots, N$.

In (4), the MCA density is a weighted linear combination of an infinite number of Gaussian densities. The first density, $m = 0$, is thought to represent the background Gaussian noise. The remaining densities, $m \geq 1$, are thought to model impulse noise. In this context, m can be seen as a noise state, i.e., $m = 0$ and $m \geq 1$ show that there is no impulse and the impulses are present, respectively. It is clear from (5) that the noise state m is a Poisson distributed random variable such that the probability of being in a given state is equal to α_m.

In most detection problems, it is often assumed that the noise samples z_k, $k = 1, \cdots, N$ are independent so that the probability density function (pdf) of each sample can be used to determine the joint pdf of $\mathbf{z} = [z_1, \cdots, z_N]$. Since the impulsive component of noise is due to interference from external sources, the samples at the consecutive sampling instants may be statistically dependent. It was shown in [17] for urban environments that, of course, the sampling spacing must be greater than an impulse mean duration to have independent samples. When the impulse mean duration is greater than the bit duration, it is possible to have dependencies between two consecutive sampling instants. Therefore, to guarantee independence between noise samples, the replicas of the transmitted signal are interleaved over time in order to break the dependencies of impulse noise[1]. Under this assumption, the joint pdf of a noise vector $\mathbf{z} = [z_1 \cdots z_k]$ is simply

$$p(\mathbf{z}) = \prod_{k=1}^{N}\sum_{m=0}^{\infty} \alpha_m g(z_k; 0, \sigma_m^2)\,. \tag{8}$$

In the following analysis, we assume that there is no memory in signals transmitted in successive signal intervals. Given the observation vector $\mathbf{r} = [r_1, \cdots, r_N]$, we are going to review the previously studied detectors of binary signal in the presence of MCA noise.

B. Optimum Detector

Assuming equiprobable transmit symbols, the optimum detector computes the test statistics

$$\Lambda(r) = \frac{\prod_{k=1}^{N} p(r_k|H_1)}{\prod_{k=1}^{N} p(r_k|H_0)} \underset{H_0}{\overset{H_1}{\gtrless}} 1\,, \tag{9}$$

where the hypotheses H_1 and H_0 correspond to transmit signals $+s(t)$ and $-s(t)$, respectively. $p(r_k|H_{1,0})$ is the conditional pdf of the observed sample given $H_{1,0}$. In [12], the optimum detector for binary signals corrupted by MCA noise is evaluated and the various theoretical bounds that quantify its

[1]Interleaving is, of course, a suboptimum approach, since the statistical bindings in the disturbance are not utilized (no noise whitening).

performance are derived. Substituting (4) into (9), we obtain the following log-LRT:

$$\ln\Lambda(r) = \ln\left(\frac{\prod_{k=1}^{N}\sum_{m=0}^{\infty}\frac{A^m}{m!\sigma_m}\mathrm{e}^{-\frac{(r_k-B)^2}{2\sigma_m^2}}}{\prod_{k=1}^{N}\sum_{m=0}^{\infty}\frac{A^m}{m!\sigma_m}\mathrm{e}^{-\frac{(r_k+B)^2}{2\sigma_m^2}}}\right)\underset{H_0}{\overset{H_1}{\gtrless}}0$$
$$= \sum_{k=1}^{N}\ln\left(\frac{\sum_{m=0}^{\infty}\frac{A^m}{m!\sigma_m}\mathrm{e}^{-\frac{(r_k-B)^2}{2\sigma_m^2}}}{\sum_{m=0}^{\infty}\frac{A^m}{m!\sigma_m}\mathrm{e}^{-\frac{(r_k+B)^2}{2\sigma_m^2}}}\right)\underset{H_0}{\overset{H_1}{\gtrless}}0\ . \quad (10)$$

The log-LRT in (10) cannot be simplified further and leads to a high computational complexity.

C. Suboptimum Detectors

Obviously, The high complexity of (10) is due to the sum of exponential functions. This differs from a maximum likelihood (ML) detection in AWGN, where the likelihood function contains only one exponential function and hence, the log-LRT reduces to a linear decision rule. As a suboptimal solution, the linear detector may be used, which is optimum in Gaussian noise. Here, the following test statistic is computed:

$$\sum_{k=1}^{N} r_k \underset{H_0}{\overset{H_1}{\gtrless}} 0\ . \quad (11)$$

However, the linear detector provides a poor performance compared with the optimum one in a predominantly impulsive channel, i.e., when $A \ll 1$. In [12], an LOD is shown to reduce the receiver complexity and provide an almost optimum performance under a small signal assumption. Using a power series expansion for small signals, i.e., for $B \approx 0$, the optimum decision rule reduces to

$$\sum_{k=1}^{N} -\frac{d}{dr_k}\ln\left(p(r_k)\right)\underset{H_0}{\overset{H_1}{\gtrless}} 0\ . \quad (12)$$

The interesting aspect of this rule is that it comprises a linear detector preceded by a logarithmic memoryless nonlinearity $-d/dr\ln(p(r))$. This receiver is optimum for small signals, but it becomes suboptimum at higher signal levels. To simplify the logarithmic nonlinear function and remove the dependence on an MCA density, a clipping or a blanking preprocessor can be used [13]. In [15], [16], it has been shown that (4) can be approximated by a maximum value of the first three terms when the impulsive index A is sufficiently small. Hence, the MCA density (4) becomes

$$p(z_k) \approx \max_{m=0,1,2}\left\{\alpha_m g(z_k;0,\sigma_m^2)\right\}\ , \quad (13)$$

and accordingly, (10) can be represented as [15], [16]

$$\ln\Lambda(r) \approx \sum_{k=1}^{N}\left(\max_{m=0,1,2}\left\{l_m(r_k|H_1)\right\} - \max_{m=0,1,2}\left\{l_m(r_k|H_0)\right\}\right)\ , \quad (14)$$

where

$$l_m(r_k|H_1) = -\frac{(r_k-B)^2}{2\sigma_m^2} + \ln\left(\frac{\alpha_m}{\sigma_m}\right)\ , \quad (15)$$

$$l_m(r_k|H_0) = -\frac{(r_k+B)^2}{2\sigma_m^2} + \ln\left(\frac{\alpha_m}{\sigma_m}\right)\ , \quad (16)$$

and $(r_k \mp B)^2$ is the distance metric between the received observation r_k and the possible transmitted one $\pm B$. The terms $\ln(\frac{\alpha_m}{\sigma_m})$, $m = 0, 1, 2$, are bias terms due to unequal variances σ_m and noise state probabilities α_m. This detector requires less complexity than the optimum one. However, it still needs to compute $l_m(r_k|H_{1,0})$, $\forall m = 0, 1, 2$.

III. Approximated ML Detector with Reduced Complexity

As we show in (4), the MCA density is expressed as a weighted infinite sum of Gaussian densities with different variances. This leads to a complex realization of the optimum detector (10). From (5), we can show that the noise state probability α_m tends to zero as m approaches infinity. Therefore, the infinite sum may be truncated to a finite sum. The formula of (13) relies on a three term approximation of the MCA density. The suboptimum detector that applies this approximation is equivalent to a log-sum representation, i.e., $\ln\left(\sum_m \alpha_m g(z;0,\sigma_m^2)\right)$ can be approximated by $\max_m\{\ln(\alpha_m g(z;0,\sigma_m^2))\}$. Selecting the maximum term is equivalent to determining the noise state m given A and Γ [18]. It has been shown in [14] that for a wide range of A and Γ, the Gaussian mixture model provides a sufficiently accurate approximation of (4) as follows:

$$p(z_k) \approx \overbrace{\alpha_0 g(z_k;0,\sigma_0^2)}^{\text{Gaussian term}} + \overbrace{\alpha_1 g(z_k;0,\sigma_1^2)}^{\text{impulsive term}}\ , \quad (17)$$

where $\sigma_0^2 = \frac{N_0}{2}\cdot\frac{\Gamma}{1+\Gamma}$ and $\sigma_1^2 = \frac{N_0}{2}\cdot\frac{\frac{1}{A}+\Gamma}{1+\Gamma}$ In this model, we have two noise states only, i.e., $m = 0$ and $m = 1$ corresponding to a Gaussian and impulsive an state, respectively. The terms $\alpha_0 = \mathrm{e}^{-A}$ and $\alpha_1 = 1 - \mathrm{e}^{-A}$ represent the noise state probabilities [19]. According to (17), when A becomes very small, e.g., $A \to 10^{-2}$, the probability of being in the Gaussian state will be higher than that of the impulsive state. However, the impulsive term cannot be ignored since its variance σ_1^2 becomes very large compared with the variance of the Gaussian term σ_0^2. This scenario is used to model a strongly impulsive channel. When A grows large (asymptotically, $A \to \infty$, although $A \cong 10$ already represents a large value of A), the probability of the Gaussian state approaches zero, $e^{-A} \to 0$. Thus, the noise pdf can be approximated by the "impulsive" term alone, which has a Gaussian density with variance $\sigma_1^2 \approx \frac{N_0}{2}\cdot\frac{\Gamma}{1+\Gamma}$.

Using a log-sum approximation, the Gaussian mixture model of impulse noise can be approximated to a maximum term of the noise states. Our task in this part is to determine a simple method to estimate the noise state at the receiver. Hence, we can detect if the received sample is affected by either Gaussian noise or impulsive noise. To illustrate this point, Fig. 2 depicts the MCA density and the pdfs of Gaussian and impulsive states of noise. From this figure, the MCA density can be further approximated as

$$p(z) \approx \begin{cases}\alpha_0 g(z;0,\sigma_0^2) & \text{if } -z_0 \le z \le +z_0\\ \alpha_1 g(z;0,\sigma_1^2) & \text{otherwise}\ ,\end{cases} \quad (18)$$

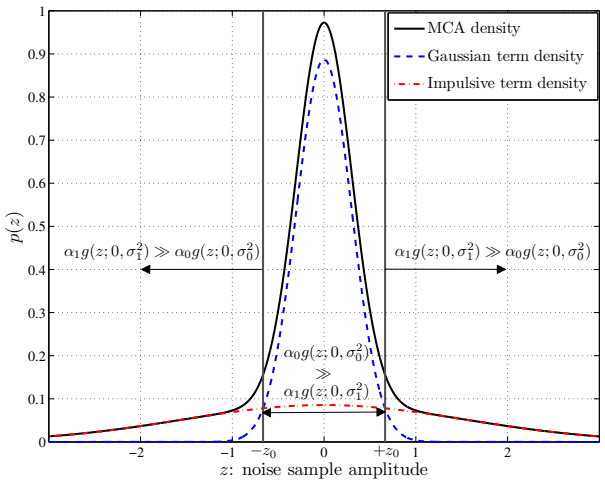

Fig. 2. The MCA density and the pdfs of Gaussian and impulsive states of a Gaussian mixture model for $A = 0.4$ and $\Gamma = 0.1$.

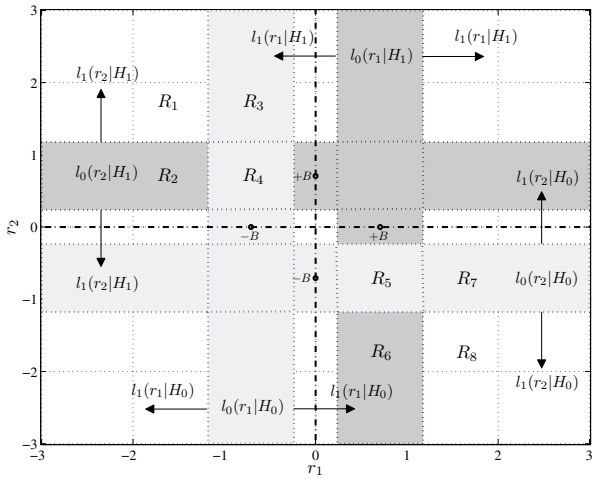

Fig. 3. The overlap regions of binary signals in MCA noise.

where $\pm z_0$ denotes the threshold for discriminating the state of noise, and it can be obtained as

$$\alpha_0 g(z_0;0,\sigma_0^2) = \alpha_1 g(z_0;0,\sigma_1^2)\ , \tag{19}$$

thus,

$$\frac{\mathrm{e}^{-A}}{\sqrt{2\pi\sigma_0^2}}\mathrm{e}^{-\frac{z_0^2}{2\sigma_0^2}} = \frac{1-\mathrm{e}^{-A}}{\sqrt{2\pi\sigma_1^2}}\mathrm{e}^{-\frac{z_0^2}{2\sigma_1^2}}\ . \tag{20}$$

We obtain

$$z_0 = \sqrt{\frac{2\sigma_0^2\sigma_1^2}{\sigma_1^2-\sigma_0^2}\ln\left(\frac{\sigma_1\mathrm{e}^{-A}}{\sigma_0(1-\mathrm{e}^{-A})}\right)}\ , \tag{21}$$

and hence, the log-LRT in (14) can be rewritten as follows:

$$\ln\Lambda(r) = \sum_{k=1}^{N}\{l(r_k|H_1) - l(r_k|H_0)\} \underset{H_0}{\overset{H_1}{\gtrless}} 0\ , \tag{22}$$

where

$$l(r_k|H_1) = \begin{cases} l_0(r_k|H_1)\,, & \text{if } -z_0 \le r_k - B \le z_0 \\ l_1(r_k|H_1)\,, & \text{otherwise} \end{cases}\ , \tag{23}$$

$$l(r_k|H_0) = \begin{cases} l_0(r_k|H_0)\,, & \text{if } -z_0 \le r_k + B \le z_0 \\ l_1(r_k|H_0)\,, & \text{otherwise} \end{cases}\ . \tag{24}$$

$l_m(r_k|H_1)$ and $l_m(r_k|H_0)$ are as given in (15) and (16), respectively. Furthermore, (22) can be simplified further for a given number of observations, N, as we will show in the next section for $N = 2$.

IV. Decision Boundary Analysis

Evaluating the decision regions is a new approach for analyzing the operation of the optimum and suboptimum detectors for binary signals in the presence of SαS noise [20]. Up to now, there has been no investigation how the decision regions of the optimum detector in the presence of MCA noise should look like. In this section, we examine the behavior of the optimum detector by introducing the decision boundary analysis for a two-dimensional case ($N = 2$).

Figure 3 depicts the overlap regions of received samples in a 2-dimensional space. Under hypotheses H_1 and H_0, the received samples are centered at $(+B,+B)$ and $(-B,-B)$, respectively. For each hypotheses, we use the proposed MCA density approximation (18) to express the conditional pdfs of the received samples r_1 and r_2. Therefore, the space of conditional pdfs can be divided into impulsive or Gaussian regions. Our goal is to derive the decision rules, which classify the received samples into their respective hypothesis. As we can see in Fig. 3, there are four overlap regions in the second and fourth quadrant. Since these regions are identical in both quadrants, we only present the analytical derivation for the regions in the second quadrant. The decision boundaries are calculated using the following log-LRT:

$$l(r_1|H_1) + l(r_2|H_1) = l(r_1|H_0) + l(r_2|H_0)\ . \tag{25}$$

In the overlap region R_1, the impulsive state is the dominant term of the conditional pdfs for the received samples r_1 and r_2. Then, (25) can be expressed as

$$l_1(r_1|H_1) + l_1(r_2|H_1) = l_1(r_1|H_0) + l_1(r_2|H_0)\ . \tag{26}$$

By substituting (23) and (24) into (26), the decision boundary can be solved as

$$r_2 = -r_1\ , \tag{27}$$

which is the exact boundary in AWGN (11). In the region R_2, the impulsive term is the dominant state of r_1 and r_2 for H_0. Given H_1, the impulsive and Gaussian terms are the states of r_1 and r_2, respectively. Inserting (23) and (24) into (25) again, yields

$$r_1 = \frac{\sigma_0^2-\sigma_1^2}{4B\sigma_0^2}\left(k_0^2 - (r_2^2 - br_2 + B^2)\right)\ , \tag{28}$$

where $b = 2B\frac{\sigma_0^2+\sigma_1^2}{\sigma_1^2-\sigma_0^2}$. In the region R_3, we obtain

$$r_2 = \frac{\sigma_1^2-\sigma_0^2}{4B\sigma_0^2}\left(k_0^2 - (r_1^2 + br_1 + B^2)\right)\ , \tag{29}$$

and finally, in R_4, we have

$$r_2 = -r_1\ , \tag{30}$$

$$r_2 = r_1 + b\ . \tag{31}$$

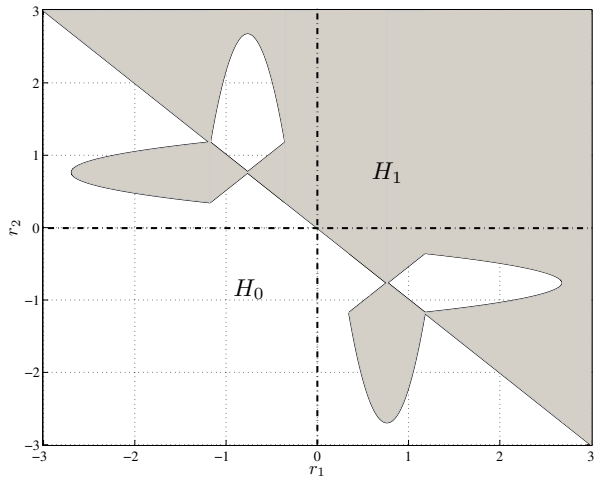

Fig. 4. Proposed decision regions with $A = 0.4$, $\Gamma = 0.1$ at an $\mathrm{SNR} = 0$ dB for $B = 1/\sqrt{2}$. Shaded area: decide for H_1, white area: decide for H_0.

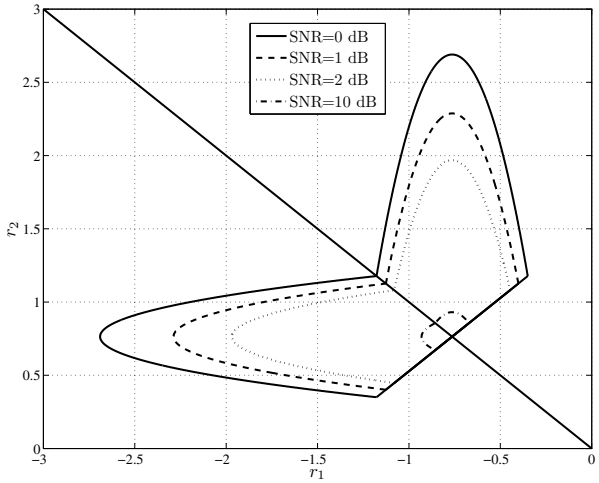

Fig. 6. Decision regions at different SNR values for $A = 0.4$ and $\Gamma = 0.1$.

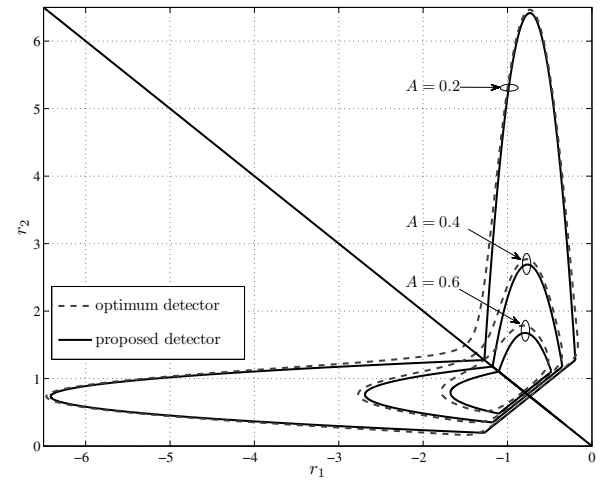

Fig. 5. Decision regions of the proposed and optimum detectors for different values of an impulsive index A with $\Gamma = 0.1$ at an $\mathrm{SNR} = 0$ dB.

Based on the above analysis, the decision boundaries of the proposed detector are illustrated in Fig. 4 for $A = 0.4$ and $\Gamma = 0.1$. We can see that the proposed detector has disjoint nonlinear decision boundaries, which was expected, since the impulse noise generally leads to nonlinear structures.

In order to examine the decision regions of the proposed detector, we compare them with those obtained from the ML ratio test (10). Since the exact evaluation of the optimum decision regions is complicated, we solve (10) numerically to draw the exact regions. Figure 5 illustrates this comparison in the second quadrant for different values of the impulsive index A. We observe that the proposed detector provides a good approximation of the exact optimum decision regions. Therefore, we can say that the proposed detector behaves almost as the optimum one by exploring the most likely regions that are caused by impulse noise. Furthermore, from this figure, we can analyze the behavior of the optimum receiver for different values of A. On the one hand, for small A, the received noise exhibits strong impulsiveness, the nonlinear boundaries become larger. On the other hand, as A increases, the nonlinear regions move closer to the linear boundary, which justifies why the linear detector performs like the optimum one at large values of A.

V. Performance Analysis of Suboptimum Detectors

In this section we employ the decision boundary analysis to evaluate the behavior of suboptimum detectors such as a linear detector and an LOD.

A. Linear Detector

In [12], the performance of the linear detector is evaluated in the presence of MCA noise. There has been no clear justification, yet, why it performs poorly as A becomes small. The linear receiver has one linear decision boundary, as given by (27) and hence it ignores a wide area of nonlinear regions, which result from the impulsive character of the noise distribution. It is clear from Fig. 5 that as the impulsiveness increases, the nonlinear regions become larger, which increases the error probability of the linear receiver. The expected performance of the linear detector can be evaluated by plotting the decision regions at different values of a signal-to-noise ratio (SNR). As shown in Fig. 6, when the SNR increases, the nonlinear regions move closer to the linear regions. This illustrates why, at high SNRs, the optimum receiver does not perform much better than the linear receiver for $N \leq 10$ [12].

B. Locally Optimum Detector

The LOD [12] represents a practical realization of the optimum detector when the signal amplitude is small, or equivalently at low SNR values. Based on our evaluation, we introduce another view for appraising the behavior of the LOD. That is, the decision boundaries of the LOD (evaluated numerically) are plotted and compared with those of the proposed detector to deduce its behavior at different SNRs. Figure 7 depicts the decision boundaries for $A = 0.6$ and $\Gamma = 0.1$ (we only show the regions of the second quadrant). As we can see from this figure, at a small signal level ($\mathrm{SNR} = -6$ dB), there is more than a 60% overlap between

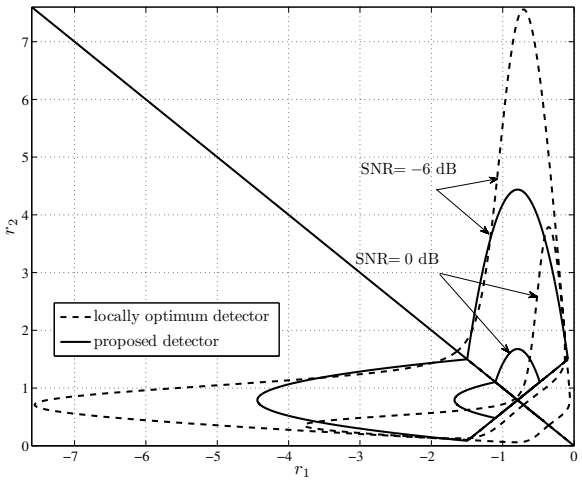

Fig. 7. Decision regions for the proposed detector compared with the LOD at different values of SNR with $A = 0.6$ and $\Gamma = 0.1$.

the two regions, and subsequently the LOD has almost the same performance as our proposed one. At a higher signal level (SNR $= 0$ dB), the LOD nonlinear region deviates completely from the proposed one. As a result, the LOD will not correctly detect the received signal in these regions.

VI. Clipping Nonlinearity with Adaptive Thresholds

It has been shown in [13] that the nonlinearity operation of the LOD can be approximated by a clipping preprocessor in the presence of MCA noise. The clipping detector simply consists of a linear detector preceded by a clipping device. Hence, it has a simple structure and adds almost no complexity to the linear detector. The clipping operation limits the signal amplitudes to a given maximum value γ. However, the performance improvements introduced by the clipping nonlinearity strongly depend on the choice of that threshold. The threshold optimization has been considered in several publications [21]–[23] for a Gaussian mixture and an MCA noise model. The idea behind the optimization principle of [21] is to maximize the SNR at the output of a clipping device. Unfortunately, this solution does not guarantee a closed-form analytical expression for the optimum γ even for the simple Gaussian mixture model. In [22], [23], the threshold optimization problem is carried out for a binary PSK with a multicarrier modulation scheme. The optimum threshold is selected to discriminate samples affected by impulses and impulse-free samples for a large number of subcarriers. Here, we applied this approach to a single carrier binary PSK scheme. For a given threshold γ, the conditional probability of detection P_d is the probability of the received sample, corrupted only by impulse noise, to exceed γ. The conditional probability of false alarm P_f is the probability of the received signal, corrupted by Gaussian noise, to exceed γ. Under the hypothesis H_1, P_d and P_f are thus given by

$$P_d(\gamma) = 2\int_{\gamma}^{\infty} g(r; B, \sigma_1^2)dr = \operatorname{erfc}\left(\frac{\gamma - B}{\sqrt{2\sigma_1^2}}\right) , \qquad (32)$$

$$P_f(\gamma) = 2\int_{\gamma}^{\infty} g(r; B, \sigma_0^2)dr = \operatorname{erfc}\left(\frac{\gamma - B}{\sqrt{2\sigma_0^2}}\right) , \qquad (33)$$

with

$$\operatorname{erfc}(x) = \frac{2}{\sqrt{\pi}}\int_{x}^{\infty} \exp(-x^2)dx \, . \qquad (34)$$

In [23], two optimization criteria are suggested to derive the optimum thresholds. In the first criterion (combination criterion), the optimum threshold γ_c^* satisfies

$$\gamma_c^* = \arg\max\left\{P_d - P_f\right\} \, . \qquad (35)$$

Hence, this function can easily be maximized with respect to a clipping threshold γ to yield the solution

$$\gamma_c^* = B + \sqrt{\frac{2\sigma_0^2\sigma_1^2}{\sigma_1^2 - \sigma_0^2}\ln\left(\frac{\sigma_1}{\sigma_0}\right)} \, . \qquad (36)$$

In the second criterion (Siegert criterion), the noise state probabilities $(1 - \mathrm{e}^{-A})$ and e^{-A} are weighed in the combination of P_d and P_f, respectively. The optimum threshold γ_s^* should satisfy

$$\gamma_s^* = \arg\max\left\{(1 - e^{-A})P_d - e^{-A}P_f\right\} \, . \qquad (37)$$

This yields

$$\gamma_s^* = B + z_0 \, , \qquad (38)$$

where z_0 is defined in (21). Note that γ_s^* has the same solution of the proposed upper threshold, see (23), to estimate the state of noise under H_1. To evaluate the performance of both criteria, the receiver operating characteristic (ROC) [23] is used to show why γ_c^* provides a better performance than γ_s^*.

A. Clipping Threshold Analysis

In [20], the performance improvements of a clipping operation are explained using decision boundaries for binary signals corrupted by SαS noise. In this section, we discuss the performance of clipping thresholds derived by the two considered criteria (combination and Siegert criterion) using the decision boundaries for binary PSK signals corrupted by MCA noise. Due to symmetry, we restrict our analysis to the second quadrant only. In this quadrant, the decision regions of the clipping nonlinearity with thresholds γ_c^* and γ_s^* in MCA noise of parameters $A = 0.4$ and $\Gamma = 0.1$ are depicted in Fig. 8. Using the threshold γ_c^*, the limiter clips all received samples in the region C_1 (shaded area) to the point $(-\gamma_c^*, \gamma_c^*)$, which is on the linear boundary. In the regions C_2 and C_3, the limiter clips the samples to the lines $r_2 = \gamma_c^*$ and $r_1 = -\gamma_c^*$, respectively. The threshold γ_s^* limits the samples in the region C_1 to a linear boundary point $(-\gamma_s^*, \gamma_s^*)$. As stated in [20], the optimum threshold should clip the nonlinear regions to a point on a linear boundary to eliminate the effect of the nonlinear decision boundary before applying a linear detector. As we can see in Fig. 8, the threshold of a combination criterion influences larger regions than the threshold of the Siegert criterion, which is in line with the result of a ROC analysis for selecting the better threshold [23].

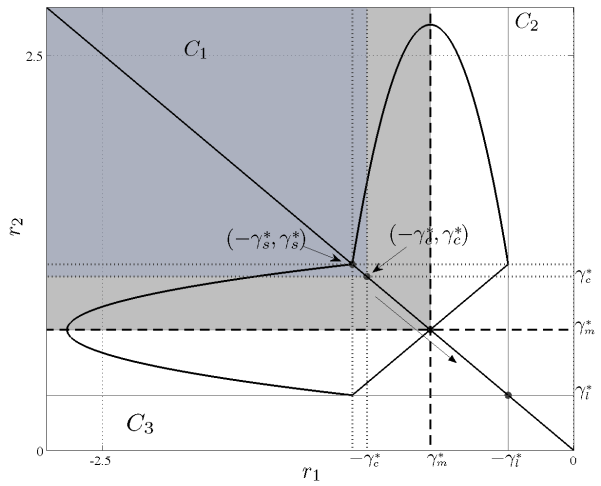

Fig. 8. The effects of clipping thresholds on the decision regions.

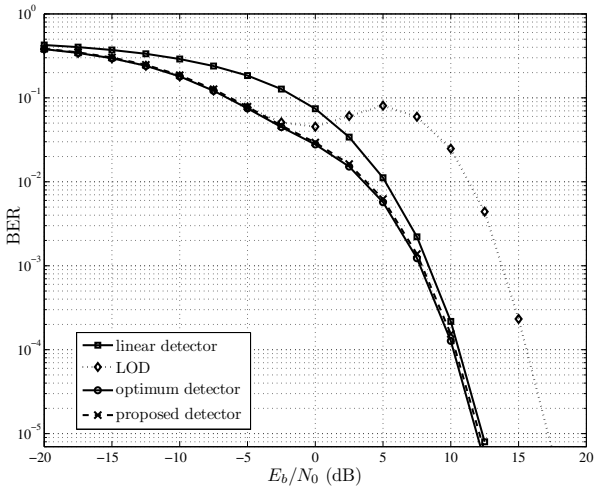

Fig. 9. Performance comparison over a weakly impulsive channel with $N = 4$.

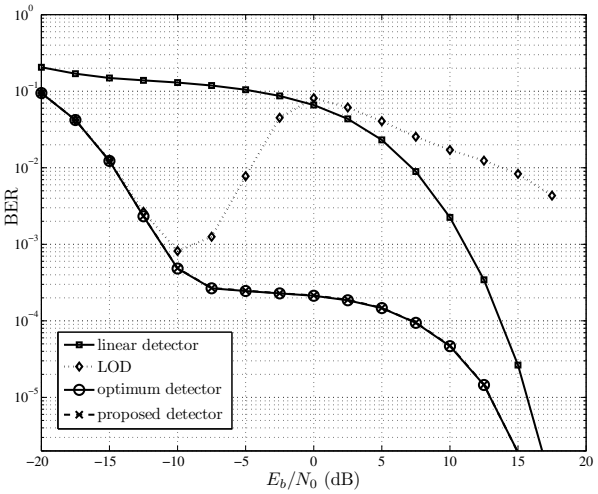

Fig. 10. Performance comparison over a moderately impulsive channel with $N = 4$.

B. Threshold Assignment using Decision Boundaries

As shown in Fig. 8, moving the clipping threshold down along the linear boundary limits a large area of nonlinear regions, which subsequently improves the performance of the concatenated linear detector. To completely prevent nonlinear regions, one may select the threshold at the point $(-\gamma_l^*, \gamma_l^*)$, which can be calculated analytically as the intersection point of (29) and (31) to be

$$\gamma_l^* = B - z_0 + \frac{4B\sigma_0^2}{\sigma_1^2 - \sigma_0^2} \, . \tag{39}$$

However, this threshold clips the correct regions inside C_2 and C_3 as well. To keep the impact on the other decision regions at an acceptable level, we propose the threshold at the intersection point, $(-\gamma_m^*, \gamma_m^*)$, which limits the largest area of the nonlinear regions without affecting the correct regions. Using (30) and (31), the threshold γ_m^* can be derived as

$$\gamma_m^* = B\frac{\sigma_0^2 + \sigma_1^2}{\sigma_1^2 - \sigma_0^2} \, . \tag{40}$$

With this threshold, we can limit half of the nonlinear regions to the point $(-\gamma_m^*, \gamma_m^*)$ on the line $r_2 = -r_1$. The other half will be limited to the lines $r_1 = -\gamma_m^*$ or $r_2 = \gamma_m^*$ as shown in Fig. 8. Since the points of the linear boundary $r_2 = -r_1$ are assigned (detected) randomly to H_1 or H_0, the proposed threshold will not offer a significant performance improvement when $N = 2$. It is expected as N increases, the probability of having unclipped samples (reliable samples) will be increased, which releaves the effect of clipped samples at the linear detector.

VII. Simulation Results

In this section, we present a series of simulation results to illustrate the bit-error ratio (BER) of antipodal signals with rectangular pulses for the proposed detectors in different impulse noise environments. In all simulations, we assume that the detectors have a priori knowledge of the exact noise parameters. This is a reasonable assumption, since it has been shown that reliable estimates can be extracted from samples of noisy data [18], [24] and can be applied in real communication systems. Figures 9, 10, and 11 show the BER of the proposed detector, the optimum detector, the LOD, and the linear detector with $N = 4$ in different MCA channels. To simulate these channels, we use three sets of impulse noise parameters: a weakly impulsive channel with $(A, \Gamma) = (0.5, 0.1)$, a moderately impulsive channel with $(A, \Gamma) = (0.1, 0.01)$, and a strongly impulsive channel with $(A, \Gamma) = (0.01, 0.01)$, respectively, which are within the specified range of A and Γ [24].

In a weakly impulsive channel, the optimum detector does not offer a significant improvement over a linear detector. This was expected, since in this channel case, the optimum decision boundaries are close to those of the linear detector. In figures 10 and 11, we see that the proposed detector behaves as the optimum one. Moreover, we observe the performance degradation of the LOD at a high SNR, which supports our justification in Section IV. At high SNRs, the LOD assumes incorrect decision boundaries for impulsive regions. Therefore, it has a much worse performance than that of a linear detector. In addition, the performance improvement of the optimum detector over the linear detector decreases

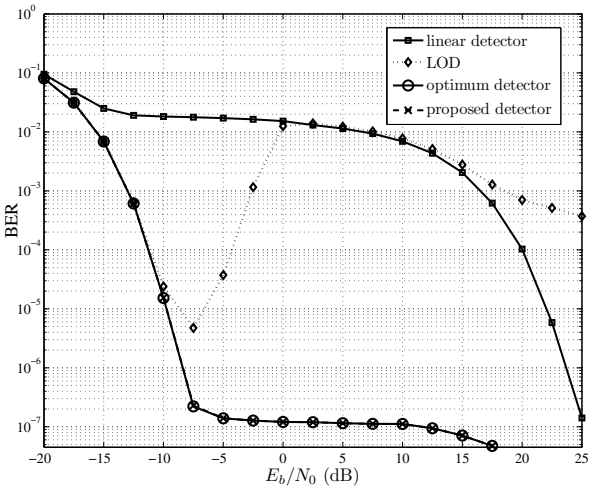

Fig. 11. Performance comparison over a strongly impulsive channel with $N = 4$.

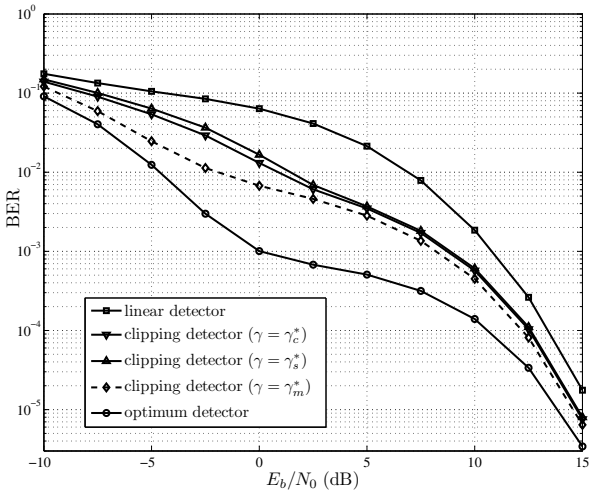

Fig. 12. BER performance of a clipping detector with the proposed thresholds for $N = 4$.

as the SNR increases. This result corroborates our analysis that the nonlinear decision regions of the optimum receiver is diminishing at high SNRs.

We also compared the performance of a clipping detector that uses the proposed threshold, $\gamma = \gamma_m^*$ as given in (40), with those based on a combination and a Siegert criterion. An MCA channel with parameters $A = 0.1$ and $\Gamma = 0.1$ is used. Figures 12 and 13 show the results for $N = 4$ and $N = 8$, respectively. Our results depict the performance improvements introduced by a clipping operation over a linear detector. Furthermore, we observe that the limiter that uses the proposed threshold, $\gamma = \gamma_m^*$, has a better performance than the other thresholds, which is in accordance with our analysis of Section V. In Fig. 13, there is an improvement of about 3.5 dB for the proposed threshold over the threshold of a combination criterion at a BER of 10^{-4}. This illustrates that the clipping detector with the proposed threshold offers a very good performance at almost no additional complexity over a linear detector. It is worth mentioning that although the proposed threshold was derived when $N = 2$, it gives a substantial improvement for $N = 4$ and $N = 8$. The reason

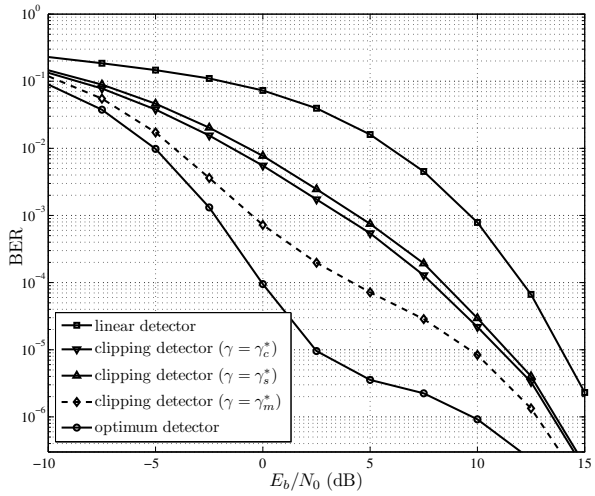

Fig. 13. BER performance of a clipping detector with the proposed thresholds for $N = 8$.

for this improvement comes from the fact that, for statistically independent noise samples, the probability of having more than two samples clipped is rather small. Of course, for very large N, the threshold value has to be re-optimized.

VIII. Conclusion

In this paper, we considered a binary signal detection in the presence of Middelton Class-A (MCA) noise. To reduce the optimum detector complexity, we proposed a further approximation of the MCA density by extracting the noise states at the receiver. Using this model, the log-likelihood function is further simpilfied. We derived a closed-form expression of the proposed detector for two independently received observations ($N = 2$) by evaluating its decision boundaries. We showed that the proposed decision boundaries provide an accurate approximation of the optimum decision regions (evaluated numerically) in different noise environments. Based on this analysis, we provided a solid explanation of the behaviors of many suboptimum detectors, including a linear detector, a locally optimum detector (LOD), and a clipping detector. A threshold optimization of the clipping detector based on a decision boundary analysis has been investigated in a new closed form.

The simulation results have shown that the bit-error ratio (BER) of the proposed detector has an almost optimum performance in several impulsive channels. It has been confirmed by simulation that the limiter that uses the proposed threshold provides better BER performance than those based on false alarm and good detection trade-off optimization.

Acknowledgment

This work is funded by the German Research Foundation (Deutsche Forschungsgemeinschaft, DFG).

References

[1] K. L. Blackard, T. S. Rappaport, and C. W. Bostian, "Measurements and models of radio frequency impulsive noise for indoor wireless communications," *IEEE J. Sel. Areas Commun.*, vol. 11, no. 7, pp. 991–1001, Sep. 1993.

[2] O. Z. Batur, M. Koca, and G. Dundar, "Measurements of impulsive noise in broad-band wireless communication channels," in *Proc. 2008 IEEE Conf. Ph.D. Research Microelectron. Electron.*, pp. 233–236.

[3] D. Middleton, "Statistical-physical models of electromagnetic interference," *IEEE Trans. Electromagn. Compat.*, vol. EMC-19, no. 3, pp. 106–127, Aug. 1977.

[4] M. Nassar, K. Gulati, A. K. Sujeeth, N. Aghasadeghi, B. L. Evans, and K. R. Tinsley, "Mitigating near-field interference in laptop embedded wireless transceivers," in *Proc. 2008 IEEE Conf. Acoust., Speech Signal Process.*, pp. 1405–1408.

[5] Y. Xueshi and A. P. Petropulu, "Co-channel interference modeling and analysis in a Poisson field of interferers in wireless communications," *IEEE Trans. Signal Process.*, vol. 51, no. 1, pp. 64–76, Jan. 2003.

[6] K. Gulati, B. L. Evans, J. G. Andrews, and K. R. Tinsley, "Statistics of co-channel interference in a field of Poisson and Poisson-Poisson clustered interferers," *IEEE Trans. Signal Process.*, vol. 58, no. 12, pp. 6207–6222, Dec. 2010.

[7] L. Breiman, *Probability and Stochastic Processes with a View Towards Applications*. Course Technology, 1986.

[8] C. Nikias and M. Shao, *Signal Processing with Alpha-Stable Distributions and Applications*. John Wiley, 1995.

[9] J. Miller and J.'Thomas, "The detection of signals in impulsive noise modeled as a mixture process," *IEEE Trans. Commun.*, vol. 24, no. 5, pp. 559–563, May 1976.

[10] A. Tesei and C. S. Regazzoni, "The asymmetric generalized Gaussian function: a new HOS-based model for generic noise PDFs," in *Proc. 1996 IEEE Workshop Statistical Signal Array Process.*, pp. 210–213.

[11] H. Inaltekin, S. B. Wicker, M. Chiang, and H. V. Poor, "On unbounded path-loss models: effects of singularity on wireless network performance," *IEEE J. Sel. Areas Commun.*, vol. 27, no. 7, pp. 1078–1092, Sep. 2009.

[12] A. Spaulding and D. Middleton, "Optimum reception in an impulsive interference environment—part I: coherent detection," *IEEE Trans. Commun.*, vol. 25, no. 9, pp. 910–923, Sep. 1977.

[13] S. Rappaport and L. Kurz, "An optimal nonlinear detector for digital data transmission through non-Gaussian channels," *IEEE Trans. Commun. Technol.*, vol. 14, no. 3, pp. 266–274, June 1966.

[14] K. Vastola, "Threshold detection in narrow-band non-Gaussian noise," *IEEE Trans. Commun.*, vol. 32, no. 2, pp. 134–139, Feb. 1984.

[15] D. Umehara, H. Yamaguchi, and Y. Morihiro, "Turbo decoding in impulsive noise environment," in *Proc. 2004 IEEE Global Telecommun. Conf.*, pp. 194–198.

[16] S. Miyamoto, M. Katayama, and N. Morinaga, "Optimum detection and design of TCM signals under impulsive noise environment," in *Proc. 1992 IEEE International Conf. Syst. Eng.*, pp. 473–478.

[17] A. D. Spaulding, "Amplitude and time statistics of urban manmade noise," in *Proc. 1971 International Commun. Conf.*, pp. 8–13.

[18] J. Yu-Zhong, H. Xiu-lin, L. Wen-Lu, and Z. Shu-Xia, "Estimation of two-dimensional Class A noise model parameters by Markov chain monte carlo," in *Proc. 2007 IEEE International Workshop Comput. Adv. Multi-Sensor Adaptive Process.*, pp. 249–252.

[19] K. F. McDonald and R. S. Blum, "A statistical and physical mechanisms-based interference and noise model for array observations," *IEEE Trans. Signal Process.*, vol. 48, no. 7, pp. 2044–2056, July 2000.

[20] T. S. Shehata, I. Marsland, and M. El-Tanany, "A novel framework for signal detection in alpha-stable interference," in *Proc. 2010 IEEE Veh. Technol. Conf.*, pp. 1–5.

[21] S. V. Zhidkov, "Analysis and comparison of several simple impulsive noise mitigation schemes for OFDM receivers," *IEEE Trans. Commun.*, vol. 56, no. 1, pp. 5–9, Jan. 2008.

[22] G. Ndo, P. Siohan, M.-H. Hamon, and J. Horard, "Optimization of turbo decoding performance in the presence of impulsive noise using soft limitation at the receiver side," in *Proc. 2008 IEEE Global Telecommun. Conf.*, pp. 1–5.

[23] G. Ndo, P. Siohan, and M.-H. Hamon, "Adaptive noise mitigation in impulsive environment: application to power-line communications," *IEEE Trans. Power Delivery*, vol. 25, no. 2, pp. 647–656, Apr. 2010.

[24] S. M. Zabin and H. V. Poor, "Efficient estimation of Class A noise parameters via the EM algorithm," *IEEE Trans. Inf. Theory*, vol. 37, no. 1, pp. 60–72, Jan. 1991.

Khodr A. Saaifan Born in Lebanon 1978, received B.Sc. degree in Electrical and Electronics Engineering (with honors) from Benha Faculty of Engineering, Benha University, Egypt, in 2001, and the M.Sc. degree in Communications from Cairo University, Giza, Egypt, in 2005. Between the years 2005 and 2009, he was with the Research and Development Department at the Egyptian Telephone Company as a wireless communication engineer. He is currently pursuing his Ph.D. studies at Jacobs University Bremen. His current research interest includes impulse noise mitigation, multiple-input multiple-output (MIMO) systems, fading channels, and multicarrier modulation.

Werner Henkel Werner Henkel was born in Gelnhausen, Germany, in 1960. He received his Diploma and Dr.-Ing. (Ph.D.) degree from Darmstadt University of Technology (TUD) in May 1984 and June 1989, respectively. From 1989 to 1999 he was with Deutsche Telekom's R&D Labs in Darmstadt and on sabbatical leave at AT&T Bell Laboratories (later Lucent) in 1993/94. From 1999 to 2002 he was with the newly founded Telecommunications Research Center Vienna, heading a basic research group dealing with access technologies with a focus on signal processing and coding for DSL. In August 2002, Dr. Henkel was appointed professor for telecommunications at the University of Applied Sciences in Bremen. Since September 2003 he is a professor for electrical engineering at the Jacobs University Bremen. Earlier teaching obligations were at University of Kaiserslautern and TU Vienna.

He was a guest editor for the June 2002 issue of IEEE JOURNAL ON SELECTED AREAS IN COMMUNICATIONS. He was in the program/organizating committees of ISIT 1997, the International Zürich Seminar 2004, of EUSIPCO 2004 and 2007, ICC 2006, and of the Turbo Symposia 2008, 2010, and 2014. Publications are in the areas of coding, iterative decoding, coded modulation, network coding, frame synchronization, channel modeling, impulse noise, DSL, single- and multicarrier transmission, and MIMO/multiuser systems. Current research activities have a focus on unequal error protection in networking, coding, and physical layer, multicarrier transmission, MIMO and multiuser systems, iterative decoding, channel measurement and modeling, and gene coding.